Rapid Communications

## Rotating magnetic nanorods detect minute fluctuations of magnetic field

Vaibhav Palkar,\* Pavel Aprelev,\* Arthur Salamatin, Artis Brasovs, Olga Kuksenok, and Konstantin G. Kornev Department of Materials Science and Engineering, Clemson University, South Carolina 29634-0971, USA

(Received 11 January 2019; published 13 November 2019)

Magnetic nanorods rotating in a viscous liquid are very sensitive to any ambient magnetic field. We theoretically predicted and experimentally validated the conditions for two-dimensional synchronous and asynchronous rotation as well as three-dimensional precession and tumbling of nanorods in an ambient field superimposed on a planar rotating magnetic field. We discovered that any ambient field stabilizes the synchronous precession of the nanorod so that the nanorod precession can be completely controlled. This effect opens up different applications of magnetic nanorods as sensors of weak magnetic fields, for microrheology, and generally for magnetic levitation.

DOI: 10.1103/PhysRevE.100.051101

When a ferromagnetic nanorod with a magnetic moment **m** is suspended in a liquid of viscosity  $\eta$  and a uniform rotating magnetic field **B** is applied, the nanorod experiences a magnetic torque that aligns the nanorod with the field and a viscous drag torque which is much stronger than the torque caused by the nanorod inertia. Planar rotation of an applied field causes two distinct regimes of the in-plane nanorod motion. If the field rotation frequency  $\omega$  is below a certain critical value, the nanorod moves synchronously with the field; due to viscous drag torque, its magnetic moment lags the field by a constant angle  $\psi$  (see Fig. 1). The greater the rotation frequency  $\omega$ , the larger is the angle  $\psi$  [1,2]. At a critical frequency  $\omega_C = mB/\Gamma$ , where  $\Gamma$  is the rotational drag coefficient [discussed later and in the Supplemental Material (SM) Sec. S4.2 [3]], the nanorod aligns perpendicularly to the field and reaches its terminal angular velocity of rotation. At  $\omega > \omega_C$ , the field rotates faster than the nanorod, switching the regime of rotation from a synchronous to an asynchronous one. Hence, magnetic torque cannot be kept constant and, as a consequence, the nanorod motion gains an oscillatory component [1,2]. The in-plane asynchronous rotation of a ferromagnetic nanorod in a planar rotating magnetic field was considered predictable and has been reliably used for many microrheological applications [4-13]. Magnetic rotational spectroscopy (MRS) [4-7] takes advantage of this characteristic oscillatory feature of rotation of inertialess rods to characterize the rheological properties of fluids. It has been claimed that such a nanorod—with the fixed magnetic moment m collinear with its geometric long axis—should remain in the plane of a rotating magnetic field and exhibit no out-of-plane rotation [14]. This statement seems to be prevailing in the literature and this motion has been discussed thoroughly [4-12,15]. However, during experimental observations, even a nanorod beginning its rotation in plane, after a long enough time, would always come out of plane and puzzle the experimentalist [16].

The phenomenon of out-of-plane motion is extremely detrimental to an experimentalist attempting to use MRS for an accurate rheological measurement. Especially as the probe size decreases from millimeters to hundreds of nanometers and the probe magnetic moment drops down drastically [17], the effect of the ambient field, e.g., the Earth's magnetic field, becomes significant. The component of this ambient field orthogonal to the plane of rotation could alter the magnetic torque to push the nanorod out of the original plane of rotation. This study aims at understanding the effects of constant out-of-plane microtesla bias fields on these dynamics. Caroli and Pincus [18] were the first to predict the possibility of the out-of-plane dynamics of magnetic particles subjected to a weak rotating planar field biased by a strong field. The problem in question is significantly different: The Earth's field may be comparable with the applied rotating field [19]. Recently, our group [16] reported that Ni nanorods with a magnetic moment parallel to the nanorod long axis [20] go out of plane during MRS experiments. The Cimurs-Cebers theory [21] of nanorod precession caused by the deviation of the magnetic moment from the easy axis (geometric long axis) falls short to explain these observations [16]. We hypothesized that the ambient field caused this out-of-plane motion of the nanorods. We develop a theory to explain the out-of-plane motion and verify the theoretical predictions with experimental results by tracking the three-dimensional (3D) rotation of the rods in a controlled 3D magnetic field. We first describe the experimental observations and then formulate the theoretical model. We then investigate the impact of the rotation frequency of the applied field and the magnitude of the out-of-plane bias field on the out-of-plane dynamics of rotating nanorods and illustrate the applications of the obtained results to rheology.

A magnetic stage developed previously [16] was used to first cancel any ambient field and then generate the in-plane rotating magnetic field with a controlled out-of-plane bias magnetic field (Fig. 1). We report two intriguing results: continuous precession of a nanorod forced to move by a rotating field **B** in the absence of any bias field,  $\mathbf{h} = \mathbf{0}$  [Fig. 1(a)], and with small bias fields,  $\mathbf{h} \neq \mathbf{0}$  [Fig. 1(b)].

The experimental phenomena are quantified by tracking the 3D rotation of ferromagnetic Ni nanorods (mass

<sup>\*</sup>These authors contributed equally to this work.

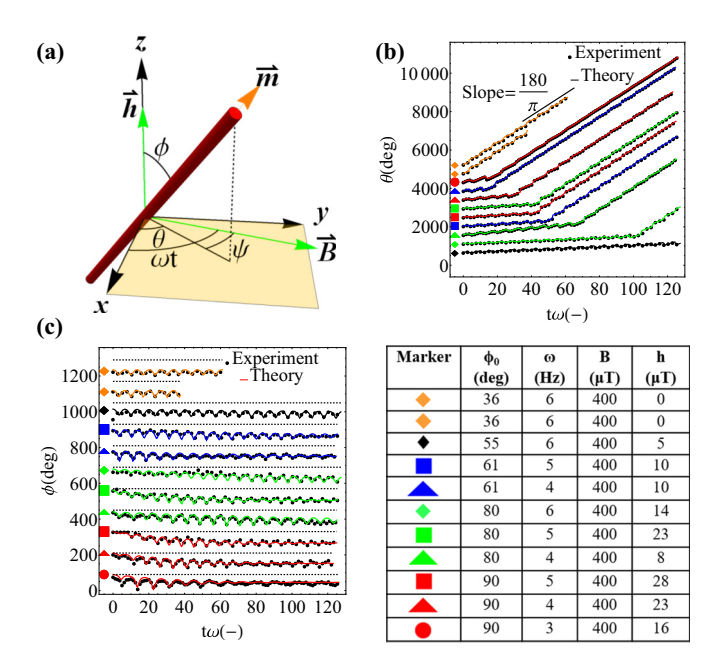


FIG. 1. (a) System of coordinates and angles used for the description of nanorod dynamics. See explanation of symbols in the text. Time evolution of (b) in-plane and (c) out-of-plane angles for the rotation of nanorods above a critical frequency ( $\omega_C \sim 2.17\,\text{Hz}$ ) in the presence of no or small bias fields ( $\mu=0-0.06$ ). Offsets were added to the data for visibility. Rods were initially oriented in plane at  $\theta_0=90^\circ$  and several different out-of-plane angles ( $\phi_0$ ). These rods were then subjected to rotating fields of different frequencies. (Information corresponding to each trajectory is in the table.) The average slopes of the trajectories in the synchronous region are  $\sim 180/\pi$  as the time data are normalized by corresponding rotation frequencies.

density  $\rho = 8.9 \,\mathrm{g/cc},$ magnetic moment  $1.5 \times 10^{-6} \,\mu\text{A}\,\text{m}^2$ , length  $l = 5 - 10 \,\mu\text{m}$ , and aspect ratio  $\sim$ 1/40) functionalized with polyvinylpyrrolidone following the protocol of Ref. [20] and suspended in a 60 wt % glycerol solution in water ( $\eta = 24$  mPa s). Experiments were performed on nanorods in bulk liquid; nanorods at or near an interface were not used, thus avoiding any interfacial effects. The motion of the nanorod was filmed and its projection on the focal plane of the microscope was tracked. The xy plane of a Cartesian system of coordinates was associated with the focal plane; the rotating magnetic  $\mathbf{B} = B(\cos \omega t, \sin \omega t, 0)$ —the so-called component—was applied parallel to this plane, and the bias field—the so-called out-of-plane component—was pointing in the z direction,  $\mathbf{h} = (0, 0, h)$  (Fig. 1). The magnitude of the in-plane field was fixed at  $B = 400 \,\mu\text{T}$  for all experiments. The in-plane component was rotating at a constant angular frequency  $\omega$ . making an angle  $\omega t$  with the x axis. The nanorod center was chosen to sit in the xy plane.

Simultaneously, a spherical system of coordinates was introduced to describe the current spatial orientation of the nanorod with respect to the laboratory system of xyz coordinates. The angle  $\theta$  of this spherical system of coordinates is taken between the x axis and the projection of the nanorod long axis onto the xy plane; the angle  $\phi$  is taken between the z axis and the nanorod long axis which is coincident with

the magnetic moment  $\mathbf{m}$  (Fig. 1). Table S2 in the SM [3] shows a relation between our notations and the commonly used Euler angles. A full description of the rotation of an arbitrary solid body requires an analysis of the equations of motion for all three Euler angles, however, as demonstrated in the SM [3] (Secs. S4.1 and S4.5), in our case the third angle is not needed: There is no magnetic torque forcing the nanorod to spin around its long axis. An auxiliary angle,  $\psi = \omega t - \theta$ , is introduced to describe the relative direction of the xy projection of the magnetic moment  $\mathbf{m}$  with respect to the rotating field  $\mathbf{B}$ . The protocol for measurements of the two determinants of the nanorod spatial orientation, the in-plane angle  $\theta$ , and the projection length L, is detailed in the SM [3].

To demonstrate the robustness of our experimental setup and theoretical predictions, at the beginning of experiment, we oriented the nanorod at specific angles  $\phi_0 = [90^\circ, 80^\circ, 61^\circ, 55^\circ, 36^\circ]$  by adjusting the in-plane and out-of-plane components of a constant aligning field. The initial in-plane angle  $\theta_0 = 90^\circ$  and the total magnitude of the aligning field  $B_{\text{align}} = 150 \,\mu\text{T}$  were kept constant. Once the nanorod was aligned with this field, we removed the aligning field and instantaneously superimposed the rotating field. Figure 1(b) shows the in-plane and Fig. 1(c) shows the out-of-plane components of the out-of-plane rotation of these nanorods. We also performed reference experiments where the nanorod was initially set parallel to the initial orientation of the magnetic field. The details of these experiments are outlined in the SM [3].

The initial oscillatory parts of the trajectories are reminiscent of the no-bias-field asynchronous rotation [Fig. 1(b), oscillations with a slowly increasing average] but, surprisingly, the nanorod gets synchronized later with the rotating field [Fig. 1(b), decaying oscillations with an average slope of  $180/\pi$ ]. Oscillations of both the in-plane [Fig. 1(b)] and out-of-plane angles [Fig. 1(c)] decay and reach a final synchronized state (for details, see Sec. S2 in the SM [3]). The out-of-plane angle reaches an equilibrium value depending on the frequency of the applied field (see below). It never reaches 90°, and the rod performs a stable precessional motion in sync with the rotating field. Thus, the out-of-plane dynamics with the out-of-plane bias field demonstrates a surprising synchronizing effect of the bias field. This effect deserves a detailed theoretical analysis.

Setting up the model, a unit vector  $\mathbf{r}$  along the nanorod long axis parallel to the magnetization and the angular velocity  $\boldsymbol{\omega}$  of the nanorod are defined as  $\mathbf{r} = (\sin \phi \cos \theta, \sin \phi \sin \theta, \cos \phi)$ ,  $\boldsymbol{\omega} = \mathbf{r} \times \dot{\mathbf{r}}$ . In the effective field  $\mathbf{B}_{\rm eff} = \mathbf{B} + \mathbf{h}$ , the 3D rotation of a nanorod is described by balancing the magnetic torque  $\tau_{\mathbf{M}} = \mathbf{m} \times \mathbf{B}_{\rm eff}$  and viscous torque  $\tau_{\mathbf{V}} = -\Gamma \boldsymbol{\omega}$  [22,23]. The rotational drag coefficient,  $\Gamma = \pi \eta L_0^3/[3\ln(L_0/D_0) - 2.4]$ , is a function of the rod length  $L_0$ , diameter  $D_0$ , and fluid viscosity  $\eta$ . This vector torque balance,  $\mathbf{m} \times \mathbf{B}_{\rm eff} = \Gamma \boldsymbol{\omega}$ , gives a system of two ordinary differential equations. Introducing dimensionless time as  $t^* = \boldsymbol{\omega} t$ , the vector torque balance is written in dimensionless form as (for the details, see Sec. S4.1 of the SM [3])

$$\frac{d\psi}{dt^*} = 1 - \frac{1}{\Omega} \frac{\sin \psi}{\sin \phi} = f(\psi, \phi), \quad \Omega = \frac{\omega}{\omega_C}, \tag{1a}$$

$$\frac{d\phi}{dt^*} = \frac{1}{\Omega} [\cos\phi\cos\psi - \mu\sin\phi] = g(\psi,\phi), \quad \mu = \frac{h}{B}. \quad (1b)$$

The two dimensionless parameters  $\Omega$  and  $\mu$  of the autonomous system of Eqs. (1a) and (1b) describe the oscillation frequency of the magnetic field and the relative magnitude of the out-of-plane field, respectively. In the absence of the bias field ( $\mu=0$ ) and in the limit when only the in-plane motion is considered ( $\phi=90^\circ$ ), these equations are reduced to the equations derived in Ref. [24]. The introduction of the angle  $\psi$  in Eqs. (1) and Fig. 1(a) conveniently eliminates the explicit dependence of these solutions on time.

The full analysis of the nonlinear system (1) can be done using the phase portrait method of the theory of dynamic systems [25]. The nanorod dynamics is described as a 2D flow

of fictitious particles representing one of the end points of the nanorod on the surface of a unit sphere; the flow is defined in the  $(\psi, \phi)$  plane with velocities

$$\mathbf{v} = (v_{\psi}, v_{\phi}), \quad v_{\psi} = f(\psi, \phi), \quad v_{\phi} = g(\psi, \phi).$$
 (2)

There are special, stationary points in the space, where the flow velocity of the particles goes to zero, i.e., the right-hand side of Eqs. (1) turns to zero,

$$f(\psi^S, \phi^S) = 0, \ g(\psi^S, \phi^S) = 0.$$
 (3)

Equations (3) have the following explicit solution,

$$\sin \phi^{S} = \pm \left[1 + \mu^{2} + \Omega^{2} - \sqrt{(1 + \mu^{2} + \Omega^{2})^{2} - 4\Omega^{2}}\right]^{1/2} / \sqrt{2}\Omega,\tag{4a}$$

$$\sin \psi^S = \Omega \sin \phi^S = \pm \left[1 + \mu^2 + \Omega^2 - \sqrt{\left(1 + \mu^2 + \Omega^2\right)^2 - 4\Omega^2}\right]^{1/2} / \sqrt{2}. \tag{4b}$$

These stationary points describe the steady rotational motion of the nanorod and specify the constant angles ( $\psi^S$ ,  $\phi^S$ ) that the nanorod makes with the in-plane component **B** of the magnetic field and with the **h** component (z axis), respectively. This synchronous solution ( $\psi^S$ ,  $\phi^S$ ) exists for any frequency of the applied in-plane rotating field and for any nonzero bias field,  $\mu = h/B \neq 0$ . Two regimes of steady rotation are distinguishable by the magnitude of the bias field and the rotation frequency: synchronous planar rotation,  $\phi^S = 90^\circ$ ,  $\mu = 0$ , and synchronous 3D precession,  $\phi^S \neq 90^\circ$ ,  $\mu \neq 0$ . The synchronous in-plane rotation of nanorods has been studied in detail in the literature [4,5,17] and hence we focus only on 3D steady precession.

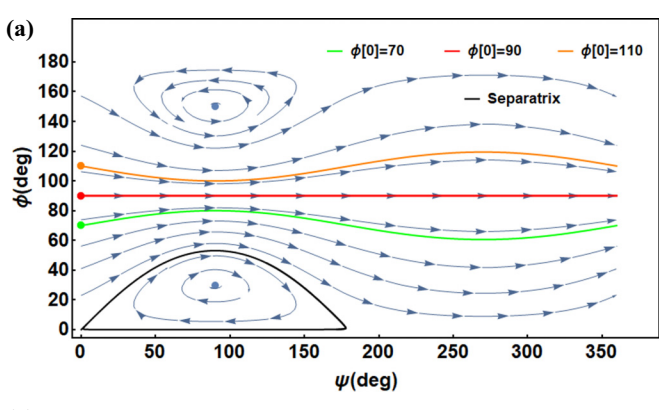
We classify the flow pattern into three parametric regions. Two of these are discussed next and the third is discussed in the SM [3] (Sec. S3.1). For the ease of perception the  $(\psi,\phi)$  space is mapped hereinafter onto the Cartesian plane. More rigorous spherical representation is discussed in the SM [3] (Sec. S4.6).

In the first parametric region ( $\Omega>1$ ,  $\mu=0$ ), two distinct flow patterns are observed: cyclic flow about the stationary points and continuous flow as demonstrated in Fig. 2 for  $\Omega=2$ ,  $\mu=0$ . The flow trajectories show different dynamics depending on the initial orientation of the nanorod. Some (red trajectory) follow the continuous flow path while others perform cyclic motion about the stationary points. These two kinds of flows are separated by the separatrix.

Nanorod trajectories are classified according to the initial orientation of the nanorod. A nanorod starting in the **B** plane  $(\phi = 90^{\circ})$ , the red trajectory in Fig. 2) would stay in the same plane and perform asynchronous motion. The red trajectory thus corresponds to the planar asynchronous motion [1,2]. For other initial orientations of the nanorods, different out-of-plane dynamics are observed [see Figs. 2(a) and 2(b)]. Figure 2(a) offers a possible explanation for the spontaneous out-of-plane motion reported in our earlier work [16]. If the nanorod experiences an isolated out-of-plane perturbation (say, at some time instant, the red trajectory in Fig. 2 gets perturbed to green or orange), the nanorod would not

asymptotically come back to the plane but continue asynchronous out-of-plane motion.

We experimentally verified the out-of-plane motion described above. The nanorod was initially tilted out of the focal plane of observation, at  $\phi = 36^{\circ}$ , and then the bias field was removed, and the in-plane rotating field was applied parallel to



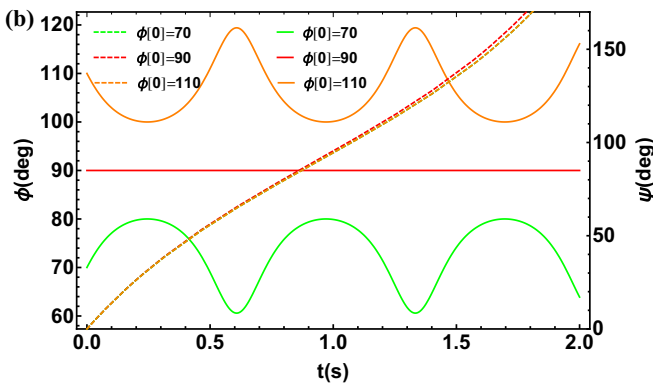


FIG. 2. (a) Phase space for the cyclic flow at  $\Omega=2$ ,  $\mu=0$ . (b) Time dependence of  $\phi$  (solid lines) and  $\psi$  (dashed lines) corresponding to the phase portrait at  $\omega=1.6$  Hz. Color (red, green, and orange) corresponds to certain initial conditions for  $\varphi$  (see legend). The initial condition for  $\psi$  is always zero.

the focal plane of observation. These trajectories are marked by orange diamonds in Fig. 1. The rotation frequency of the applied field was set above the critical rotation frequency, suggesting that asymptotically the nanorod should engage in in-plane asynchronous rotation. Surprisingly, despite the intuitive expectation that the magnetic torque  $\tau_{\mathbf{M}} = \mathbf{m} \times \mathbf{B}$ should pull the nanorod towards the focal plane, the nanorod performed oscillatory out-of-plane motion and never settled to the plane (trajectories marked orange diamonds in Fig. 1). In each cycle, when the nanorod was about to approach the focal plane, it was kicked off the plane as soon as it approached some  $\phi^C(\phi^S < \phi^C < 90^\circ)$ . Then, on its way in the vertical direction, the nanorod was again pulled back towards the rotation plane. In this manner, the nanorod never reaches an equilibrium orientation or synchronization with the magnetic field and the out-of-plane angle  $\phi$  oscillates about a mean position, never crossing the  $\phi = 90^{\circ}$  plane. This experiment demonstrates the presence of out-of-plane asynchronous dynamics without any out-of-plane field. Thus, the out-of-plane dynamics is an inherent characteristic of the planar rotating field. In light of this, one might wonder what role is played by the out-of-plane component of the field. We now analyze this by showing theoretically that switching on even a small out-of-plane field causes synchronization of the out-of-plane rotation of nanorods.

Switching on the bias field (second parametric region  $\Omega > 1$ ,  $\mu > 0$ ), the cyclic flow pattern observed in the previous regime transforms into a spiraling flow demonstrated in Fig. 3(a) for  $\Omega = 2$ ,  $\mu = 0.5$ . The two stationary points in this case become attractive and repulsive spirals. Fictitious particles, i.e., the nanorod end points, spiral away from the repulsive spiral and move toward the attractive spiral where they ultimately become stationary, though a number of 360° cycles of  $\psi$  might be necessary.

Thus, the nanorods starting from any initial condition ultimately oscillate about the synchronous angle. These oscillations decay with time, asymptotically reaching the synchronous state  $(\varphi^S; \psi^S)$  that is a function of  $(\Omega; \mu)$  in Eqs. (4). Figure 3(b) displays these oscillatory dynamics in terms of time-dependent trajectories where decaying oscillations followed by synchronization are clearly visible. The above analysis confirms that the out-of-plane precession does exist at  $\Omega > 1$  without any out-of-plane fields. Small out-of-plane fields, however, impart stability to the precessional dynamics. Next, we demonstrate the impact of the out-of-plane field and rotation frequency on the stable precession dynamics that are experimentally verified.

Theoretically, for  $\Omega < 1$ , the nanorod indefinitely rotates synchronously with the magnetic field and the effect of a small ambient field,  $\mu < 0.05$ , is not noticeable. Figure 4 shows that the stationary angle  $\phi^S$  is bound between 87° and 90°, indicating that the nanorod rotates in plane. The situation changes dramatically at  $\Omega > 1$ . For negligibly small  $\mu \ll 1$  bias field, one expects that once placed in the plane of rotation, the nanorod would keep rotating in plane. However, the expectation is not fulfilled when a small  $\mu = 0.05$  bias field is applied in our experiments. As shown by the red curve and the data points crowded at  $30^\circ < \phi^S < 50^\circ$  and  $1.25 < \Omega < 2.3$  in Fig. 4(b) in the presence of even a small bias field, one observes a drastic transition to the 3D steady precession.

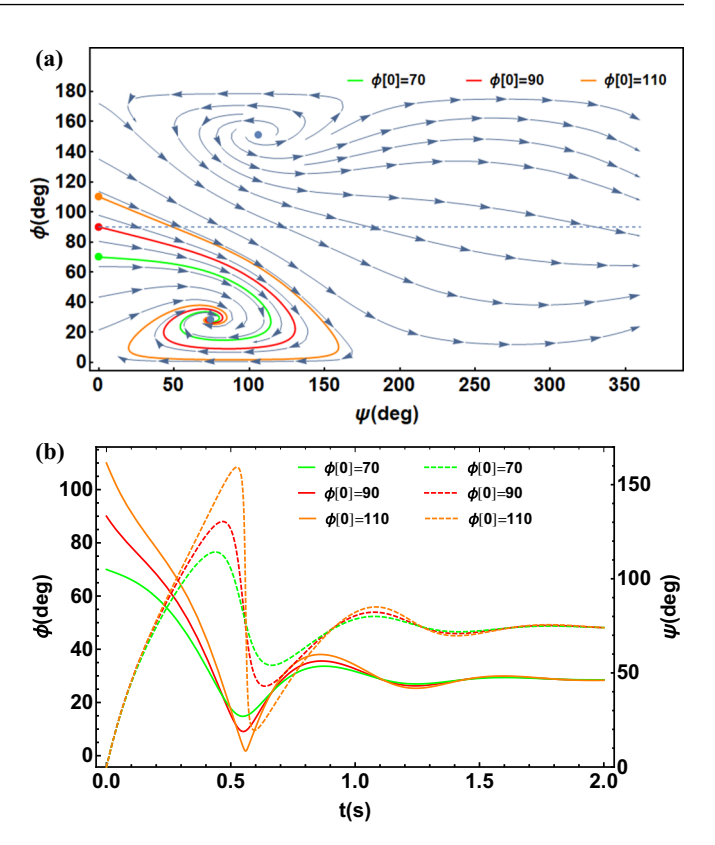


FIG. 3. (a) Phase space for the spiral flow at  $\Omega=2$ ,  $\mu=0.5$ . (b) The time dependence of the angles corresponding to the phase portrait at  $\omega=1.6\,\mathrm{Hz}$ . The dashed lines are the  $\psi$  trajectory and the solid lines are the  $\phi$  trajectory. Color (red, green, and orange) corresponds to certain initial conditions for  $\varphi$  (see legend). The initial condition for  $\psi$  is always zero.

The steady precession angle  $\phi^S$  [Eqs. (4)] is observed to significantly depend on the frequency of the applied in-plane component of the field, dropping from  $\sim 90^{\circ}$  to  $0^{\circ}$  as the frequency increases.

It is thus seen that in the applied 2D rotating magnetic field, ferromagnetic nanorods demonstrate rich dynamic behavior. Magnetic rotational spectroscopy of fluids takes advantage of only one possible scenario when the nanorods undergo a transition from synchronous to asynchronous 2D motion. However, 3D motion brings more surprises. We discovered that when the nanorod is aligned out of plane, and no bias field is present, the nanorod is first pulled towards the plane of the field rotation but then keeps tumbling, never settling in the plane of the applied rotating field. This 3D effect is purely dynamic—there is no static equivalent of this behavior: A static field will always force the nanorod to coalign with the field [17].

We also discovered that the introduction of an orthogonal bias field changes the 2D rotation scenario dramatically: The 3D nanorod motion can be synchronized with an applied rotating field of any frequency. Our work suggests that the stronger the bias field, the shorter is the time required for a nanorod to find its steady-state precession angle (SM Sec. S5 [3]). These experimental observations have been supported by the nonlinear phase portrait theory and theoretical analysis of the stability of nanorod rotation near the steady-state precession

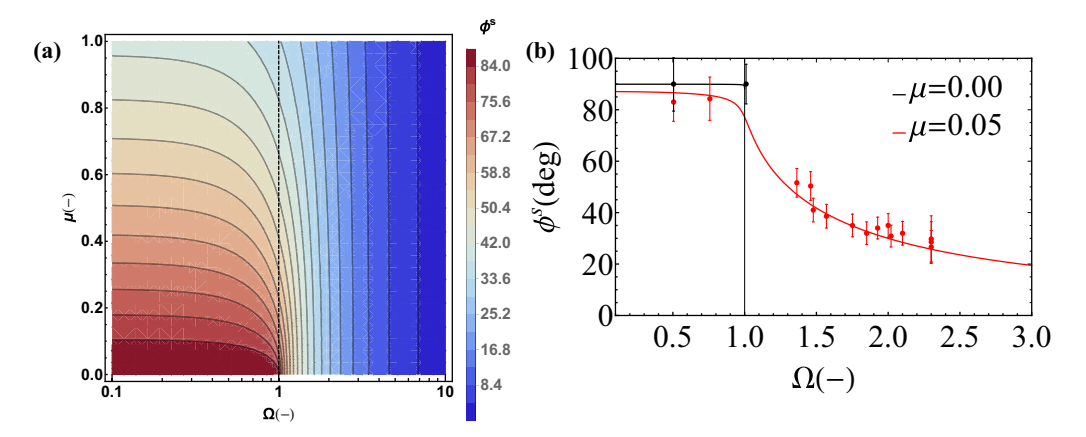


FIG. 4. (a) Contours of the steady precession angle  $\phi^S$  and (b) experimental (circles with error bars) and theoretical (lines) angles  $\phi^S$  at different rotation frequencies.

angles. The developed theory and corresponding experiments demonstrate that the out-of-plane bias field causes synchronization of the precessional dynamics. The final synchronous angle is a strong function of the field rotation frequency and therefore can be controlled precisely. We demonstrated that the obtained results can be utilized for experimental analyses of viscosity (SM Sec. S5 [3]) in microrheological applications. Utilizing fast precessional stabilization with a bias field, one will be able to analyze the viscosity of the liquid samples much easier compared to the existing methods. When the liquid in question is given only in a minute amount and the solvent evaporates fast or some chemical reactions change the

drop viscosity, the proposed procedure may help significantly. The discovered effects can be used in many other applications involving nanorheology, magnetic sensing, and the magnetic levitation of particles [26].

This work was supported in part by the National Science Foundation EPSCoR Program under NSF Award No. OIA-1655740. This research was partly supported by NASA through the SC Space Grant Consortium Graduate Assistantship, NASA Grant No. NNX15AL49H. A.S. acknowledges partial support from the Russian Government Program of Competitive Growth of Kazan Federal University.

- [1] J. Frenkel, Kinetic Theory of Liquids (Dover, New York, 1955).
- [2] P. G. de Gennes and J. Prost, *The Physics of Liquid Crystals* (Clarendon, Oxford, UK, 1993).
- [3] See Supplemental Material at http://link.aps.org/supplemental/ 10.1103/PhysRevE.100.051101 for details of experimental analysis protocols, additional experimental data, detailed theoretical derivations, and discussions thereof.
- [4] K. G. Kornev, Y. Gu, P. Aprelev, and A. Tokarev, in *Springer Book Series on Characterization Tools for Nanoscience & Nanotechnology*, edited by C. Kumar (Springer, New York, 2016).
- [5] J. F. Berret, Int. J. Nanotechnol. 13, 597 (2016).
- [6] L. Chevry, N. K. Sampathkumar, A. Cebers, and J. F. Berret, Phys. Rev. E 88, 062306 (2013).
- [7] A. Hecht, P. Kinnunen, B. McNaughton, and R. Kopelman, J. Magn. Magn. Mater. 323, 272 (2011).
- [8] J. F. Berret, Nat. Commun. 7, 10134 (2016).
- [9] A. Tokarev, B. Kaufman, Y. Gu, T. Andrukh, P. H. Adler, and K. G. Kornev, Appl. Phys. Lett. 102, 033701 (2013).
- [10] B. H. McNaughton, R. R. Agayan, J. X. Wang, and R. Kopelman, Sens. Actuators, B 121, 330 (2007).
- [11] P. Kinnunen, I. Sinn, B. H. McNaughton, and R. Kopelman, Appl. Phys. Lett. 97, 223701 (2010).
- [12] K. V. T. Nguyen and J. N. Anker, Sens. Actuators, B 205, 313 (2014).
- [13] P. Dhar, Y. Y. Cao, T. M. Fischer, and J. A. Zasadzinski, Phys. Rev. Lett. 104, 016001 (2010).

- [14] P. Dhar, C. D. Swayne, T. M. Fischer, T. Kline, and A. Sen, Nano Lett. 7, 1010 (2007).
- [15] C. Wilhelm, F. Gazeau, and J. C. Bacri, Phys. Rev. E 67, 061908 (2003).
- [16] P. Aprelev, B. McKinney, C. Walls, and K. G. Kornev, Phys. Fluids 29, 072001 (2017).
- [17] Y. Gu and K. G. Kornev, Adv. Funct. Mater. 26, 3796 (2016).
- [18] C. Caroli and P. Pincus, Phys. Kondens. Mater. 9, 311 (1969).
- [19] A. Chulliat, S. Macmillan, P. Alken, C. Beggan, M. Nair, B. Hamilton, A. Woods, V. Ridley, S. Maus, and A. Thomson, The US/UK World Magnetic Model for 2015–2020: Technical Report, National Geophysical Data Center, NOAA (2015), doi:10.7289/V5TB14V7.
- [20] P. Aprelev, Y. Gu, R. Burtovyy, I. Luzinov, and K. G. Kornev, J. Appl. Phys. 118, 074901 (2015).
- [21] J. Cimurs and A. Cebers, Phys. Rev. E 88, 062315 (2013).
- [22] J. Burgers, Proc., Ned. Akad. Wet. 16, 113 (1938).
- [23] M. Doi and S. F. Edwards, The Theory of Polymer Dynamics, Vol. 73 (Oxford University Press, New York, 1988).
- [24] A. Ghosh, P. Mandal, S. Karmakar, and A. Ghosh, Phys. Chem. Chem. Phys. **15**, 10817 (2013).
- [25] S. H. Strogatz, Nonlinear Dynamics and Chaos: With Applications to Physics, Biology, Chemistry, and Engineering (Avalon, New York, 2014).
- [26] K. A. Baldwin, J. B. de Fouchier, P. S. Atkinson, R. J. A. Hill, M. R. Swift, and D. J. Fairhurst, Phys. Rev. Lett. 121, 064502 (2018).